

## Experimental (FT-IR & FT - Raman) and Theoretical Investigation, Electronic Properties of Quinoxaline

C.C.Sangeetha<sup>1\*</sup>, R.Madivanane<sup>2</sup>, V.Pouchaname<sup>3</sup>, R.Vijaya Prasath<sup>4</sup>

<sup>1</sup>Department of Physics, Manonmaniyam Sundaranar University, Tirunelveli, Tamilnadu, India.

<sup>2</sup>Department of Physics, Bharathidasan Government College for Women, Puducherry, India.

<sup>3</sup>Department of Chemistry, Bharathidasan Government College for Women, Puducherry, India.

<sup>4</sup>Department of Physics, Sri Manakula Vinayagar Institute of Tech, Puducherry, India.

\*Corres. author: carosangee@gmail.com

**Abstract:** The present work deals the structural and vibrational analysis of Quinoxaline molecule which is pharmaceutically and industrially important heterocyclic compound. The FTIR and FT-Raman spectra of Quinoxaline have been measured in the region of 0-3700  $\text{cm}^{-1}$  and UV-Visible spectrum also was recorded. The computations were carried out by employing DFT/B3LYP method with 6-311++G(d,p) basis set. The first order hyperpolarizability and its related properties ( $\alpha_0$ ,  $\mu$  and  $\Delta\alpha$ ) were also calculated by the finite field approach. The HOMO-LUMO energy gap, chemical hardness, corrosion inhibition were studied. The thermodynamic functions of the title compound have been performed. The observed and calculated wave numbers are found to be in good agreement with the experimental values. The experimental spectra also coincide with the theoretically constructed spectra. From our study we find that the title compound is a good NLO material and posses corrosion inhibition character.

**Keywords:** FT-IR & FT – Raman, Electronic Properties of Quinoxaline.

### 1. Introduction

The quinoxaline is a nitrogenous heterocyclic compound which is widely used in various industries like pharmaceuticals, dyes etc [1]. In pharmaceutical fields they were used as antibiotics such as echinomycin, levomycin and antileutin [1-7] and also play an effective role as anti-virus, anti- HIV and anti-depression as the oxidation of Nitrogen atoms of quinoxaline ring significantly increases the biological activity of the compound. Quinoxaline combination of 1,4-di-N-Oxide inhibits TB progression with 99 to 100% efficiency. The cyano-substituted quinoxaline di-N-Oxide is a potential antitumor agent which selectively kills hypoxic cells [8]. Quinoxaline derivatives recently receive more and more attention of researchers since they play important role on corrosion efficiency [9-12]. Nowadays FTIR and FT-Raman spectroscopy combined with quantum chemical computations has been recently used as an effective tool in the vibrational analysis of the drug molecules [13]. Literature survey reveals that a good amount of work has been studied on the derivatives of Quinoxaline not in quinoxaline molecule. Hence we have chosen pharmaceutically important molecule quinoxaline to study vibrational behavior, NLO activity, HOMO-LUMO analysis, chemical hardness, corrosion inhibition, thermodynamic properties and Mulliken charge analysis using computation method DFT/B3LYP . UV spectra

also calculated. The all computational data of the title compound is found to be in good agreement with experimentally observed spectral data.

## 2. Experimental Details

The compound quinoxaline was purchased from Sigma Aldrich Chemicals, USA and used as such to record the FTIR, FT Raman and UV – Visible spectra. The FTIR spectrum of quinoxaline was recorded by KBr pellet on a Burkerr 1 FS 66 v Spectrometr equipped with a global source, Ge/KBr beam splitter and a TGs detector. The FT–Raman spectrum of the compound was also recorded in the range 0-3700  $\text{cm}^{-1}$  using the same instrument with FRA 106 Raman module equipped with Nd: YAG laser source. The frequencies of all sharp bands are accurate to 2  $\text{cm}^{-1}$ . The absorption spectrum of the compound was also recorded with the shimadzu UV – Visible spectrometer. The band width on half h eight is 3.0nm.

The combination of DFT calculations of chemical shifts, frontier molecular orbital energies and harmonic vibrations with UV –Visible and IR/ Raman experimental parameters, respectively have been accepted technique to gather insight into the complete molecular structure. The novelty of our work resides in correlating the theoretically predicted optimized geometrical parameters, Harmonic vibrations, Thermodynamic properties of quinoxaline with experimental FTIR, FT Raman and UV – Visible data for the first time.

## 3. Computational Details:

Using the version 8 of Gaussian 09W (revision B.01) program [8], the DFT calculation of the title compound was carried out on Intel Core2Duo/2.20 GHz processor. Becke-3-Lee-Yang-Parr (B3LYP) functional [14-15] were used to carry out ab initio analysis with the standard 6-311 ++G (d,p) basis sets. For the simulated IR and Raman spectra pure Lorentzian band shapes with the band width of 10  $\text{cm}^{-1}$  was employed using the Gabedit Version 2.32 [16]. The animation option of the Gauss view 05 graphical interface for Gaussian program was employed for the proper assignment of the title compound and it was also used to visualize vibrational modes of the title compound and to check whether the mode was pure or mixed[17-24]. The idea of using multiple scale factors in the recent literature, had been adopted for this study and it minimized the deviation between the computed and the experimental frequencies. Vibrational frequencies are scaled with the scaling factors 0.99 for B3LYP to account for systematic errors caused by basics set incompleteness neglect of electron correlation and vibrational anharmonicity. After scaled with scaling factor, the deviation from the experiments is less than 10 $\text{cm}^{-1}$  with a few exceptions. The mean polarizability properties of quinoxaline were obtained from the theoretical calculations to show the NLO property of the molecule. The thermodynamic properties of quinoxaline such as heat capacity, entropy, and enthalpy were investigated for the different terms from the vibrational frequency calculations of title molecule. The energy of highest occupied molecular orbit ( $E_{\text{HOMO}}$ ) and the energy of Lowest unoccupied Molecular Orbital ( $E_{\text{LUMO}}$ ) the dipole moment ( $\mu$ ), the ionization potential (I), the electron affinity (A), the electro negativity (X), the global hardness ( $\eta$ ) were calculated.

## 4. Result and discussion:

### 4.1 Molecular geometry

The optimized structural parameters such as bond length, bond angle and dihedral angle for the energetically preferred geometry of quinoxaline determined by B3LYP method with 6-311++G(d,p) basis are presented in Table 1. The schematic optimized structure of quinoxaline along with the numbering is shown in Fig1. The maximum number of potentially active observable fundamentals of non linear molecule which contains N atoms is equal to (3N-6) apart from three translational and three rotational degrees of freedom [25]. From the table1, we find that if the electronegativity of the central atom decreases, the bond angle decreases. All the dihedral angles approaches  $\pm 180^{\circ}$  or  $0^{\circ}$  which indicates that the optimized structure is non planar. The bond lengths between carbon and nitrogen atoms are lesser than the remaining bonds may be due to the influence of two nitrogen atoms on the molecular str uture.

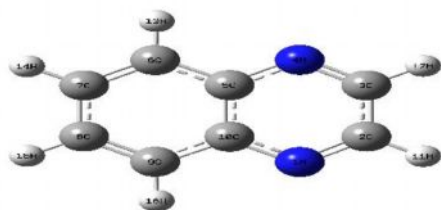


Fig 1 : The molecular structure of quinoxaline

Table 1: Optimized geometrical parameters of quinoxaline obtained from B3LYP (6-311++G) density functional calculations.

Parameters	DFT(B3LYP) 6-311++G(d,p)	Parameters	DFT(B3LYP) 6-311++G(d,p)
<b>Bond length (Å)</b>		<b>Bond angle (°)</b>	
N1-C2	1.3126	C2-N1-C10	116.528
N1-C10	1.3625	N1-C2-H11	122.5103
C2-C3	1.4202	N1-C2-C3	117.5038
C2-H11	1.0871	C3-C2-H11	119.9859
C3-N4	1.3126	C2-C3-N4	122.5103
C3-H12	1.0871	C2-C3-12	119.9858
N4-C5	1.3625	N4-C3-H12	117.5039
C5-C6	1.417	C3-N4-C5	116.5278
C5-C10	1.4293	N4-C5-C6	119.6601
C6-C7	1.374	N4-C5-C10	120.9619
C6-H13	1.0835	C6-C5-C10	119.378
C7-C8	1.4174	C5-C6-C7	119.9406
C7-H14	1.0841	C5-C6-H13	118.0434
C8-C9	1.374	C7-C6-H13	122.016
C8-H15	1.0841	C6-C7-C8	120.6814
C9-C10	1.417	C6-C7-H14	119.9583
C9-H16	1.0835	C8-C7-14	119.3603
		C7-C8-C9	120.6813
		C7-C8-H15	119.3604
		C9-C8-H15	119.9583
		C8-C9-C10	119.9405
		C8-C9-H16	122.016
		C10-C9-H16	118.0434
		N1-C10-C5	120.9617
		N1-C10-C9	119.6602
		C5-C10-C9	119.3782

#### 4.2 Vibrational and spectral analysis:

The distribution of 42 normal modes of Quinoxaline which have been performed on the recorded FT-IR and FT-Raman spectra based and the theoretically predicted wave numbers by DFT with B3LYP-6-311++G(d,p) basis sets are presented in Table 2. The calculated infrared and Raman wave numbers were well correlated with the intensities of the observed fundamental modes. The FTIR and FT-Raman spectra from both experimental and theoretical methods are shown in Fig 2.

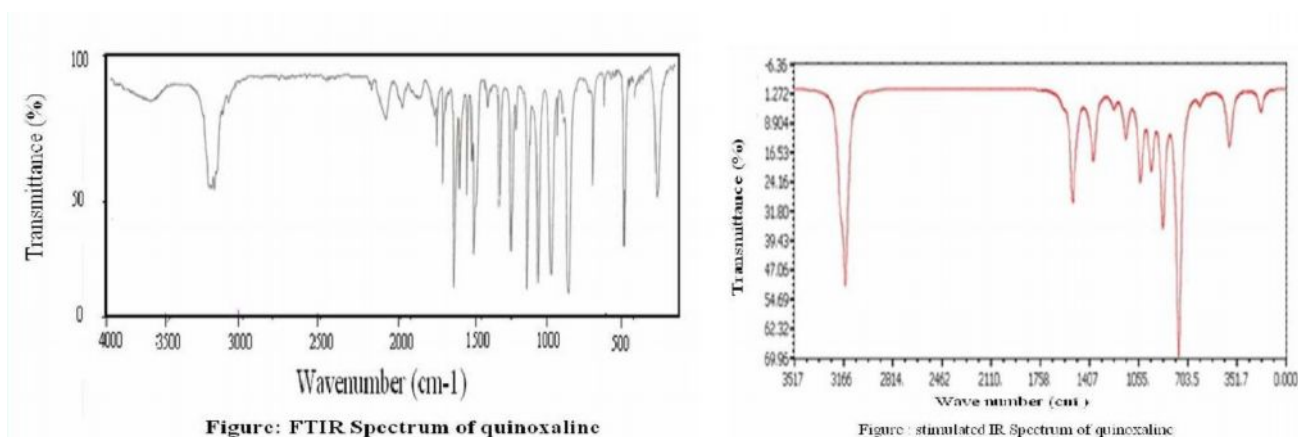


Fig 2 (a): Experimental and Theoretical FTIR spectrum.

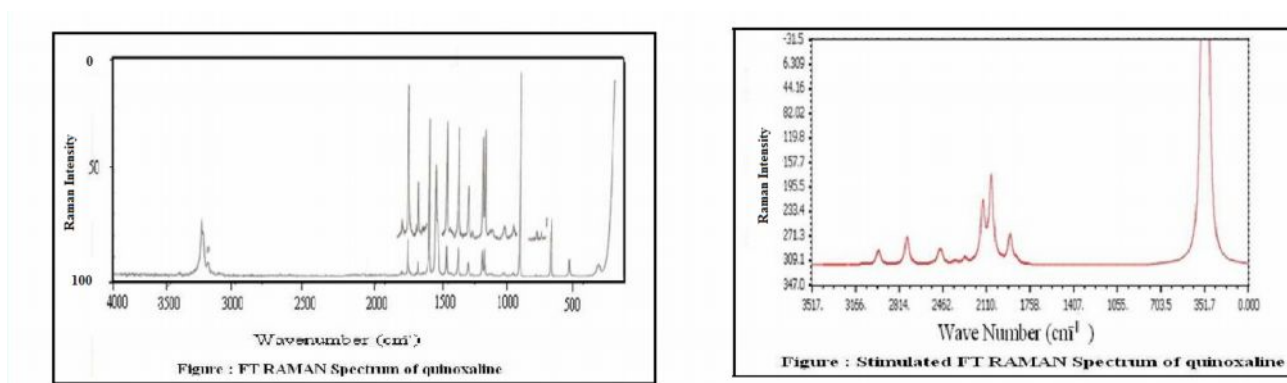


Fig 2 (b): Experimental and Theoretical FT Raman spectrum.

The aromatic compounds shows the presence of the C-H stretching vibrational around  $3100-3000\text{ cm}^{-1}$  range which is the characteristic region for the ready identification of C-H stretching vibrations [26]. C-H stretching vibrations are found in FTIR spectrum at 3128,3183,3190,3219 and in FT-Raman 3140,3155,3212 are shows good agreement with the observed wave numbers. C-H rocking vibration is found  $754\text{ cm}^{-1}$  in FT-Raman. The out of plane bending vibration of HCCH is observed in FT-Raman spectrum at  $954\text{ cm}^{-1}$ , this shows good agreement with the calculated wavenumber at  $965\text{ cm}^{-1}$ . Similarly the HCCC out of plane bending vibrations are found at  $959\text{ cm}^{-1}$  in raman spectrum. In our present molecule the C-C stretching vibrations are verified at  $1030,1385,1418,1535,1609\text{ cm}^{-1}$  in FTIR and in FT-Raman spectrum they were observed at  $1611\text{ cm}^{-1}$ . The C-C bending vibrations computed at  $170,182,412\text{ and }535\text{ cm}^{-1}$  by HF method shows an excellent agreement with the medium FT-IR band at  $196,408\text{ cm}^{-1}$  in FTIR and at  $188,534\text{ cm}^{-1}$  in FT-Raman spectrum. In the present work, the bands occurring at  $640\text{ and }804\text{ cm}^{-1}$  in FT-Raman and at  $761\text{ cm}^{-1}$  in FTIR are assigned to C-C-C in-plane bending and these assignments are in line with the earlier workers [27,28].

The identification of C-N stretching frequencies is a rather difficult task, since the mixing of vibrations is possible in this region. The C-N stretching vibration is usually a lie in the region  $1400-1200$  [29]. In our present study, the C-N stretching is observed at  $1260,1458,1494,1651\text{ cm}^{-1}$  in FT-Raman,  $1535,1609$  in FTIR spectrum respectively. The NCH bending vibrations at  $1134$  in FTIR and at  $1167$  in FTR shows good agreement with the theoretical values at  $1147,1161\text{ cm}^{-1}$ . In our present study ring twisting vibrations were observed at  $839$  in FTIR and at  $868,1009\text{ cm}^{-1}$  in FTR. The theoretically scaled values of ring deformation exactly correlates with experimental observation in FTIR at  $541,868$  and at  $975\text{ cm}^{-1}$  in FTR.

**Table 2: Experimental and calculated B3LYP/6-311++G(d,p) level vibrational frequencies ( $\text{cm}^{-1}$ ), IR Intensity ( $\text{KM Mol}^{-1}$ ), Raman Activity ( $\text{\AA}^4 \text{amu}^{-1}$ ) of Quinoxaline.**

of vibratio	Observed frequency		Calculated frequency By B3LYP/6-311++G(d,p)				Assignment
	IR	RAMAN	Unscaled	Scaled	IR Intensity	Raman Intensity	
1	196		170.3143	170.3143	0	0.2249	C-C bending
2		188.945	182.7739	182.7739	5.8364	0.1108	C-C-C opb+ C-C bending
3	400.828	399.172	399.0538	399.0538	5.4985	0.0097	C-C-C opb
4	408.422		412.6808	408.554	10.8459	2.2479	C-C bending
5	470.6		471.4394	471.4394	0	0.0059	C-C-C opb
6	493.348		499.3005	494.3075	0.0206	0.01	
7		534.133	535.6624	524.9492	0.0003	13.4678	C-C bending
8	541.18		544.0546	538.6141	0.1619	9.4107	Ring deformation
9	608.775	604.209	618.3541	618.3541	3.0074	0.3762	Ring symmetry
10	667.859	640.544	647.357	640.8834	0	0.2634	C-C-C ipb
11		754.742	769.4534	754.0643	4.6035	42.9924	C=C sym str+C-H rocking
12	761.123		771.8155	764.0973	63.6009	0.1193	C-C-C ipb+CCN bending
13	801.557	801.459					
14		804.054	806.6692	798.6025	0	0.0241	C-C-C ipb+ CCN bending
15	839.382	832.604	849.8184	832.822	0.6673	0.1129	Ring twistng
16		868.939					
17		868.939	883.6617	865.9885	32.7287	0.0818	Ring deformation
18	871.051		885.8531	868.136	0	0.0514	Ring twistng
19		920.847					
20	954.449	954.588	965.6418	955.9854	15.3522	0.9975	OpbHCCH+ring 2 twisting
21		959.778	978.8967	978.8967	0	0.2138	HCCC opb+ring 2 twisting
22		975.351	982.3209	982.3209	3.2176	0.3916	Ring deformation
23		1009.09	1000.4569	1000.457	0	0.3275	Ring twistng
24		1024.66	1029.1959	1025.144	1.2942	13.2719	CNC bending
25	1030.27		1046.0655	1029.196	20.9056	14.6285	HCC scissoring+CC sym.str
26	1134.31	1133.67	1147.5721	1136.096	10.2265	2.4233	NCH bend+CCH ipb
27		1167.41	1161.2275	1161.228	1.7534	2.754	NCH bend+CCH ipb
28		1258.25	1235.3329	1210.626	3.3739	1.9043	CCH ipb
29	1262.16	1260.84	1236.6001	1236.6	0.4485	7.6888	C-N str+CCH ipb
30	1289.83	1286.8	1289.8154	1289.815	0.2487	0.4605	CCH ipb
31		1325.1	1324.514	1324.514	0.1067	2.6548	CCH ipb
32	1385.5		1380.4913	1366.686	17.0836	88.9932	C-C sym .str+ CCH ipb
33	1418.09	1411.38	1410.5689	1410.569	2.6598	0.0571	C-C sym .str+ CCH ipb
34	1466.19	1458.09	1447.9596	1447.96	0.8657	131.989	C-N str+ CCH ipb
35	1498.21	1494.43	1498.4896	1498.49	3.5819	1.927	C-N str+ CCH ipb
36	1535.31		1529.6965	1529.697	27.9365	3.6196	C-C sym .str+ C-N str+ CCH ipb
37	1609.26		1600.4739	1600.474	2.833	36.7392	C-C sym .str+ C-N str+ CCH ipb
38		1611.22	1603.7948	1603.795	0.0001	7.5639	CC sym.str
39	1651		1653.1025	1620.04	0.3408	6.0503	C=C sym .str+ C-N str
40	3128.01		3138.34	3106.957	3.0319	89.5823	C-H str
41		3140	3155.0997	3155.1	42.3149	312.743	C-H str
42		3155	3169.3004	3169.3	2.1492	53.6151	C-H str
43	3183.23		3181.3589	3181.359	5.7419	124.307	C-H str
44	3190.16		3193.7393	3193.799	8.6194	33.6584	C-H str
45	3219.93	3212.58	3198.1736	3198.174	9.737	315.468	C-H str

sym .str –symmetric stretching, str-stretching, ipb-In plane bending, opb-Out of plane bending.

### 4.3 NLO Analysis

NLO is an important concept in current research scenario because of its vast applications in telecommunications, optical switching and signal processing [30-33]. The first-order hyperpolarizability ( $\beta_0$ ) of this novel molecular system and the related properties ( $\alpha_0$  and  $\Delta\alpha$ ) of quinoxaline were calculated using B3LYP with 6-311++G (d,p) basis set, based on the finite field approach. In presence of an applied electric field, the energy of a system is a function of the electric field. The first hyper polarizability is a third-rank tensor that can be described by a  $3 \times 3 \times 3$  matrix. The 27 components of the 30 matrix can be reduced to 10 components due to the Kleinman symmetry[34]. The components of  $\beta_0$  are defined as the coefficients in the Taylor series exponents the energy in the external electric field. When the external electric field is weak and homogeneous, this expansion becomes

$$E = E^0 - \mu_\alpha F_\alpha - 1/2 \alpha_{\alpha\beta} F_\alpha F_\beta - 1/6 \beta_{\alpha\beta\gamma} F_\alpha F_\beta F_\gamma + \dots$$

where  $E^0$  is the energy of the unperturbed molecules,  $F_\alpha$  is the field at the origin and  $\mu_\alpha$ ,  $\alpha_{\alpha\beta}$  and  $\beta_{\alpha\beta\gamma}$  are the components of dipole moment, polarizability and the first-order hyperpolarizabilities respectively. The total static dipole moment ( $\mu$ ), the mean polarizability ( $\alpha_0$ ), the anisotropy of the polarizability ( $\Delta\alpha$ ) and the mean first-order hyperpolarizability ( $\beta_0$ ), using the x, y, z components they are defined as follows:

The total static dipole moment

$$\mu = (\mu_x^2 + \mu_y^2 + \mu_z^2)^{1/2}$$

$$\alpha_0 = 1/3 (\alpha_{xx} + \alpha_{yy} + \alpha_{zz})$$

$$\beta_0 = (\beta_x^2 + \beta_y^2 + \beta_z^2)^{1/2}$$

$$= [(\beta_{xxx} + \beta_{xyy} + \beta_{xzz})^2 + (\beta_{yyy} + \beta_{yxx} + \beta_{yzz})^2 + (\beta_{zzz} + \beta_{zxx} + \beta_{zyy})^2]^{1/2}$$

$$\Delta\alpha = [(\alpha_{xx} - \alpha_{yy})^2 + (\alpha_{yy} - \alpha_{zz})^2 + (\alpha_{zz} - \alpha_{xx})^2 / 2]^{1/2}$$

The  $\alpha$  and  $\beta$  values of the Gaussian 05 output are in atomic units (a.u) and these calculated values converted into electrostatic unit (e.s.u) ( $\alpha$  : 1 a.u =  $0.1482 \times 10^{-24}$  esu; for  $\beta$  : 1 a.u =  $8.639 \times 10^{-33}$  esu; ) and these above polarizability values of quinoxaline are listed in Table (3). To study the NLO properties of molecule the value of urea molecule which is prototypical molecule is used as threshold value for the purpose of comparison. The calculated value of dipole moment of the quinoxaline compound is found to be 0.230293674 Debye. The magnitude of the molecule hyper polarizability is one of the important key factor in NLO system. The B3LYP/6-311++G(d,p) calculated first order hyperpolarizability value ( $\beta$ ) of the quinoxaline is equal to  $1.751468116 \times 10^{-30}$  e.s.u. Total dipole moment of title molecule is smaller than urea. The polarizability of the title molecule is four times smaller than urea and the first order hyper polarizability of the same molecule is one time greater than urea. [35] ( $\mu$  and  $\alpha_0$  and  $\beta$  of urea are 1.525686 Debye,  $5.047709 \times 10^{-24}$  e.s.u and  $0.780324 \times 10^{-30}$  e.s.u respectively, obtained by B3LYP/6-311++G(d,p) method. From the resultant values we identify the title compound as a good NLO material. The low value of the dipole moment may be due to the symmetries of the title molecule. The calculated value of dipole moment is mentioned in Table 3.

**Table 3 : The calculated values of electric dipole moment, polarizability and first hyperpolarizability of quinoxaline**

Parameters (a.u)	DFT B3LYP/6-311++G(d,p)
$\alpha_{xx}$	157.977056
$\alpha_{xy}$	0.000004410407
$\alpha_{yy}$	106.99404045
$\alpha_{xz}$	0.00000201425266
$\alpha_{yz}$	-0.00000145610389
$\alpha_{zz}$	55.2873792
$\alpha_0$	106.752825a.u
	$1.582076867 \times 10^{-23}$ e.s.u
$\Delta\alpha$	88.93260486
	$1.317981204 \times 10^{-23}$ e.s.u

$\beta_{xxx}$	254.511387
$\beta_{xyy}$	0.00000438708462
$\beta_{xyx}$	-15.12213323
$\beta_{yyx}$	-0.000166745762
$\beta_{xxy}$	-0.00017192135
$\beta_{xzy}$	-0.0000776069276
$\beta_{yzy}$	-0.0000134316489
$\beta_{xzz}$	-36.6566095
$\beta_{yzz}$	-0.000188351607
$\beta_{zzz}$	-0.0000537130271
$\beta$	202.7326422 a.u
	$1.751468116 \times 10^{-30}$ e.s.u
$\mu_x$	-0.5853
$\mu_y$	-0.0000
$\mu_z$	0.0000
$\mu$ total (Debye)	0.5853

#### 4.4 Frontier molecular orbital analysis:

The Frontier orbital gap helps to characterize the chemical reactivity, chemical hardness, softness of a molecule.[35]. The highest occupied molecular orbital (HOMO) and the lowest unoccupied molecular orbital (LUMO) are known as frontier molecular orbitals (FMOs).The chemical activity of the molecule is also observed from eigen values of LUMO and HOMO and from the energy gap value calculated from it [36,37].

If the energy gap is smaller, then the molecule will be excited easily. In the present study the energy gap value is found to be less and hence if electron withdrawing groups are present in this molecule, the title molecule can show NLO activity. Consequently, the lowering of the HOMO-LUMO band gap is essentially a consequence of the large stabilization of the LUMO due to the strong electron –donor ability of the electron – donor group. From the HOMO-LUMO energy gap, one can find whether the molecule is hard or soft[38].The soft molecules are more polarizable than the hard ones because they need small energy to excitation. Lower value of energy gap will render good corrosion inhibition efficiency, because the energy to remove an electron from the last occupied orbital will be low.Lower values of the energy difference will render good inhibition efficiency, because the energy to remove an electron from the last occupied orbital will be low [39].

A molecule with a low energy gap is more polarizable and is generally associated with the high chemical activity and low kinetic stability and is termed soft molecule [40]. A hard molecule has a large energy gap and a soft molecule has a small energy gap [41]. It is shown from the calculations that Quinoxaline has the least value of global hardness (0.06102 eV) and the highest value of global softness is expected to have the highest inhibition efficiency. For the simplest transfer of electron, adsorption could occur at the part of the molecule where softness(S), which is a local property, has a highest value [42]. Quinoxaline with softness value of 16.3880 has the highest inhibition efficiency.

The atomic orbital composition of the frontier molecular orbital are sketched in Fig 4. The global hardness value of the molecule can be calculated using Koopman' theorem.[43]

$$\eta = \frac{1}{2} (\epsilon_{\text{LUMO}} - \epsilon_{\text{HOMO}})$$

The hardness has been associated with the stability of chemical system. The electron affinity can be used in combination with ionization energy to give electronic chemical potential,  $\mu = \frac{1}{2} (\epsilon_{\text{LUMO}} + \epsilon_{\text{HOMO}})$ . Chemical softness(S) =  $1/\eta$  describes the capacity of an atom or group of atoms to receive electrons and is the inverse of the global hardness [44]. The global electrophilicity index,  $\omega = \mu^2 / 2 \eta$  is also calculated and these values are listed in Table 4.

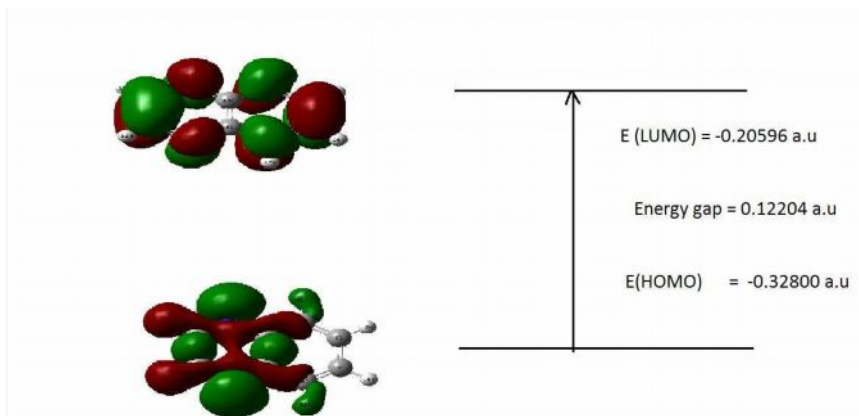


Fig 4: Atomic orbital composition of the frontier molecule for Quinoxaline.

Table 4 : Calculated energy values of Quinoxaline in its ground state.

Molecular properties	B3LYP/6-311++G(d,p)
$E_{LUMO+1}$ (eV)	-0.16108
$E_{LUMO}$ (eV)	-0.20596
$E_{HOMO}$ (eV)	-0.32800
$E_{HOMO-1}$ (eV)	-0.34654
$\Delta E_{HOMO-LUMO}$ (eV)	-0.12204
$\Delta E_{HOMO-LUMO+1}$ (eV)	-0.16692
$\Delta E_{HOMO-1-LUMO}$ (eV)	-0.14058
$\Delta E_{HOMO-1-LUMO+1}$ (eV)	-0.18546
Global hardness( $\eta$ )	0.06102
Chemical softness(S)	16.3880
Electronic chemical potential( $\mu$ )	-0.26698
Global electrophilicity index( $\omega$ )	0.58405

#### 4.6 Mullikan analysis:

In the application of quantum mechanical calculations to molecular system, the calculation of effective atomic charges plays an important role. The results are given in Table 5 .The magnitude of the carbon atomic charges found to be either positive or negative. All the hydrogen atoms have a positive charge and the two nitrogen atoms have a negative charge.

Table 5: Mulliken atomic charges of Quinoxaline for B3LYP with 6-311++G(d,p) basis sets.

S.NO	ATOMS	B3LYP/6-311++G(d,p)
1	N	-0.240463
2	N	-0.240463
3	C	0.200014
4	C	-0.016696
5	C	-0.042698
6	C	-0.011162
7	C	-0.011162
8	C	-0.042698
9	C	-0.016696
10	C	0.200014
11	H	0.023552
12	H	0.04412
13	H	0.043333
14	H	0.043333
15	H	0.04412
16	H	0.023552

#### 4.7 Thermodynamic properties

On the basis of vibrational analysis of DFT studies at 6-311++G(d,p) level, some of the thermodynamic parameters[45] are calculated. These parameters are listed out based on the statistically thermodynamic functions are given in Table 6.

**Table 6 : Theoretically computed Dipole moment(Debye), energy(au), zero point vibrational energy(kcal mol<sup>-1</sup>), entropy(cal mol<sup>-1</sup>k<sup>-1</sup>), rotational temperature(Kelvin), rotational constant(GHz), thermal energy (Kcal/Mol) and Molar capacity at constant volume(Cal/Mol-Kelvin)of Quinoxaline.**

Parameters	B3LYP/6-311++G(d,p)
Dipole moment (Debye)	0.5853
Zero point energy	323030.5 Joules/Mol
Entropy (Cal/Mol-Kelvin)	
Total	81.263
Translational	40.501
Rotational	28.811
Vibrational	11.951
Rotational temperature (Kelvin)	
	0.15252
	0.06288
	0.04452
Rotational constants (GHZ)	3.17793
	1.31020
	0.92772
Thermal Energy (KCal/Mol)	
Total	81.328
Translational	0.889
Rotational	0.889
Vibrational	79.551
Molar capacity at constant volume (Cal/Mol-Kelvin)	
Total	27.080
Translational	2.981
Rotational	2.981
Vibrational	21.118

#### 4.8 Electron absorption spectra:

Ultraviolet spectrum analysis of quinoxaline has been investigated by B3LYP/6-311++G(d,p) method. The calculated visible absorption maxima of  $\lambda_{\max}$  which is the function of the electron availability have been reported in Table 7. Molecular orbital geometry calculations shows that the visible absorption maxima of this molecule correspond to the electron transition between frontier orbitals such as transition between HOMO and LUMO. The calculated results involving the vertical excitation energies, oscillator strength (f) and wavelength are listed in table. B3LYP/6-311++G(d,p) method predict one intense electronic transition at Ev (280 nm) with an oscillator strength f= 0.0715 which is in good agreement with the measured experimental data ( $\lambda_{\text{exp}}=280$  nm) as shown in Fig 5.

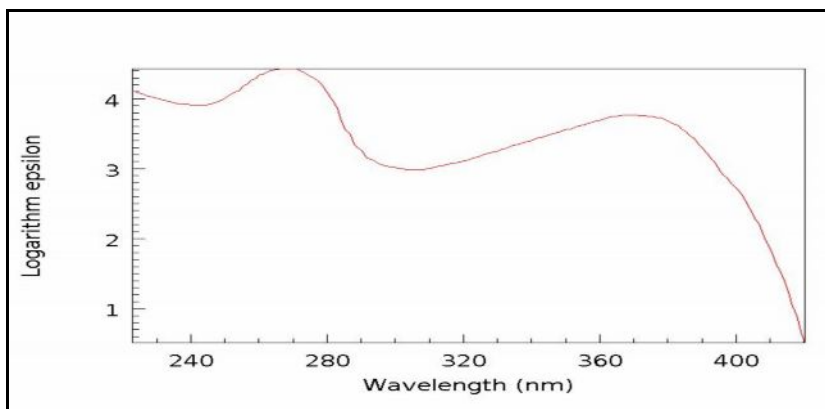


Fig 5 (a)

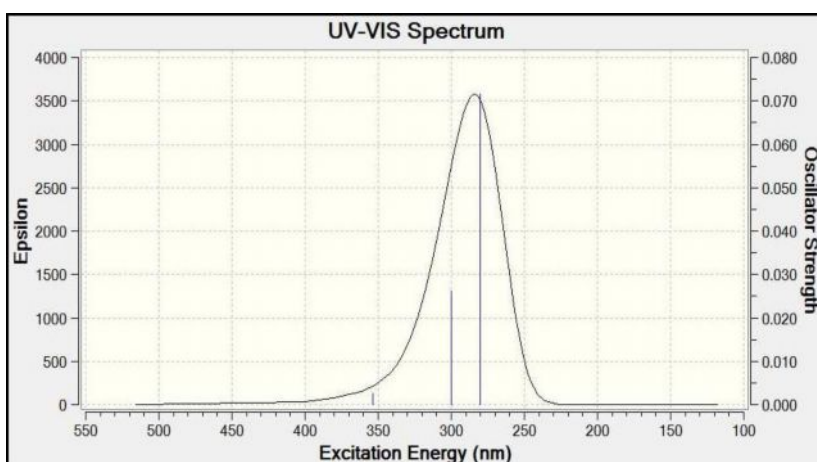


Fig 5 (b)

Fig 5: UV-Visible spectrum of Quinoxaline (a) Experimental (b) Theoretical .

**Table 7: Theoretical electronic absorption spectra of Quinoxaline (absorption wavelength  $\lambda$  (nm), excitation energies E (eV) and oscillator strengths ( f ) using DFT/B3LYP/6-311G(d,p) method in gas phase.**

Experimental		Calculated by B3LYP/6-311++G(d,p)		
$\lambda$ (nm)	Log ( $\epsilon$ )	$\lambda$ (nm)	E (eV)	(f)
353	3.5	<b>353.74</b> (33→35)	3.5050	0.0025
300	3	<b>300.41</b> (32→36) (34→35)	4.1309	0.0261
280	4.5	<b>280.05</b> (32→35) (34→36)	4.4273	0.0715

## 5. Conclusion:

The equilibrium geometries of quinoxaline were investigated and analyzed at DFT at B3LYP/6-311++G (d, p) level. The thermodynamic properties and Mullikan's charges are also analyzed. The first order hyper polarizability and low energy gap value identified that the title compound is a good NLO material. The calculated lowest Homo-Lumo energy gap value implies that the molecule was most capable of offering electrons and it could have a better performance as corrosion inhibitor. Thus from the knowledge of the physical and chemical properties of these kinds of drug materials may lead to improve the properties of the tested molecules of the drugs by applying changes of the structure.

## References:

1. <http://en.wikipedia.org/wiki/Quinoxaline>
2. Jean Renault, Michel Baron, Patrick Mailliet et al. (1981). "Heterocyclic quinones.2.Quinoxaline-5,6-(and 5-8)-diones-Potential antitumoral agents". Eur. J. Med. Chem. 16 (6): 545–550.

3. Xianghong Wu, Anne E. V. Gorden (2007). "Regioselective Synthesis of Asymmetrically Substituted 2-Quinoxalinol Salen Ligands". *J.Org. Chem.* 72(23): 8691–8699. doi:10.1021/jo701395w.PMID 17939720.
4. Z. El Adnani, M. Mcharfi, M. Sfaira, M. Benzako ura, A.T. Benjelloun, M. Ebn Touhami, *Corrosion Science* 68 (2013) 223–230.
5. Y. Abboud, A. Abourriche, T. Saffaj, M. Berrada, M. Charrouf, A. Bennamara, N.Al Himidi, H. Hannache, *Materials Chemistry and Physics* 105 (2007) 1–5.
6. I.B. Obot, N.O. Obi-Egbedi, N.W. Odozi, *Corrosion Science* 52 (2012) 923–926.
7. Synthesis of Novel Aryl Quinoxaline Derivatives by New Catalytic Methods Reza Soleymani, Neda Niakan, Shohre Tayeb, and Shirin Hakimi, *oriental journal of chemistry*, 2012, vol. 28, no. (1):pg. 687-701.
8. Photosensitization of Guanine-Specific DNA Damage by Cyano-Substituted Quinoxaline Di-N-oxide, Tarra Fuchs and Kent S. Gates, *Chem. Res. Toxicol.* 1999, 12, 1190–1194.
9. A. Zarrouk<sup>1</sup>, A. Dafali<sup>1</sup>, B. Hammouti<sup>1</sup>, H. Zarrok<sup>2</sup>, S. Boukhris<sup>2</sup>, M. Zertoubi<sup>3</sup>, *Int. J. Electrochem. Sci.*, 5 (2010) 46 – 55.
10. 12. Y. Abboud, A. Abourriche, T. Saffaj, M. Berrada, M. Charrouf, A. Bennamara, N. Al Hamidi and H. Hannache, *Mater. Chem. Phys.* 105 (2007) 1
11. 13. M. Benabdellah, R. Touzani, A. Aouniti, A. Dafali, S. Elkadiri, B. Hammouti and M. Benkaddour, *Phys. Chem. News* 36 (2007) 60
12. 14. M. Benabdellah, K. Tebbji, B. Hammouti, R. Touzani, A. Aouniti, A. Dafali and S. El Kadiri, *Phys. Chem. News*, 43 (2008) 115.
13. S. Sebastian, N. Sundaraganesan, S. Manoharan, *Spectrochim. Acta A* 74(2009)312.
14. M. J. Frisch, G. W. Trucks, H. B. Schlegel, et al., GAUSSIAN 09, Revision A.02, Gaussian, Inc., Wallingford, CT, 2009
15. A.P. Scott, L. Radom, *J. Phys. Chem.* 100 (1996) 16502–16513.
16. V. Arjunan, Arushma Raj, R. Santhanama, M.K. Marchewka, S. Mohan c, *Spectrochimica Acta Part A: Molecular and Biomolecular Spectroscopy* 102 (2013) 327–340.
17. R. Duchfield, *J. Chem. Phys.* 56 (1972) 5688–5691.
18. K. Wolinski, J.F. Hinton, P. Pulay, *J. Am. Chem. Soc.* 112 (1990) 8251–8260.
19. W.B. Tzeng, K. Narayanan, *J. Mol. Struct. (Theochem.)* 434 (1998) 247–253.
20. G. Keresztury, S. Holly, J. Varga, G. Besenyi, A. Y. Wang, J. R. Durig, *spectrochim. Acta*, 9A(1993)2007-026.
21. G. Keresztury, in: J. M. Chalmers, P. R. Griffith (Eds), *Raman spectroscopy: Theory, Hand book of vibrational spectroscopy*, vol. 1. John Wiley & Sons Ltd., New York, 2002.
22. E. D. Glendening, C. R. Landis, F. Weinhold, *WIREs Comput. Mol. Sci.* (2011) 1–42.
23. W. Kohn, L. J. Sham, *Phys. Rev.* 140(1965)A1133–A1138.
24. M. J. Frisch, G. W. Trucks, H. B. Schlegel, G. E. Scuseria, M. A. Robb, J. R. Cheeseman, G. Scalmani, V. Barone, B. Mennucci, G. A. Petersson, H. Nakatsuji, M. Caricato, X. Li, H. P. Hratchian, A. F. Izmaylov, J. Bloino, G. Zheng, J. L. Sonnenberg, M. Hada, M. Ehara, K. Toyota, R. Fukuda, J. Hasegawa, M. Ishida, T. Nakajima, Y. Honda, O. Kitao, H. Nakai, T. Vreven, J. A. Montgomery, Jr., J. E. Peralta, F. Ogliaro, M. Bearpark, J. J. Heyd, E. Brothers, K. N. Kudin, V. N. Staroverov, R. Kobayashi, J. Normand, K. Raghavachari, A. Rendell, J. C. Burant, S. S. Iyengar, J. Tomasi, M. Cossi, N. Rega, J. M. Millam, M. Klene, J. E. Knox, J. B. Cross, V. Bakken, C. Adamo, J. Jaramillo, R. Gomperts, R. E. Stratmann, O. Yazyev, A. J. Austin, R. Cammi, C. Pomelli, J. W. Ochterski, R. L. Martin, K. Morokuma, V. G. Zakrzewski, G. A. Voth, P. Salvador, J. J. Dannenberg, S. Dapprich, A. D. Daniels, O. Farkas, J. B. Foresman, J. V. Ortiz, J. Cioslowski, D. J. Fox, Gaussian, Inc., Wallingford, CT, 2009.
25. P. S. Kalsi, *spectroscopy of organic compounds*, sixth edition, p(70)
26. V. Arjunan, S. Mohan, P. S. Balamourougane, P. Ravindran, *Spectrochimica Acta Part A* 74 (2009) 1215–1223
27. G. Varsanyi, *Assignments for Vibrational Spectra of Seven Hundred Benzene Derivatives*, vol. I, Adam Hilger, London, 1974.
28. N. Syam Sundar, *Can. J. Chem.* 62 (1984) 2238.
29. M. Rangacharyulu, D. Premaswarup, *Ind. J. Pure Appl. Phys.* 16 (1978) 37.
30. Y. X. Sun, Q. L. Hao, W. X. Wei, Z. X. Yu, L. D. Lu, X. Wang, Y. S. Wang, *J. Mol. Struct.: Theochem.* 904(2009)74-82.
31. C. Andraud, T. Brotin, C. Garcia, F. Pelle, P. Goldner, B. Bigot, A. Collet, *J. Am. chem. soc.* 116(1994)2094-

2102.

32. V.M.Geskin,C.Lambert,J.L.Bredas, J.Am.chem.soc.125(2003)15651-15658
33. D.Sajan.I.H.Joe,V.S.Jayakumar,J.Zaleski,J.Mol.struct.785(2006)43-53.
34. D.A. Kleinman, Phys. Rev. 126 (1962) 1977–1979 .
35. B. Kosar, C. Albayrak, Spectrochim. Acta 78A (2011) 160–167.
36. L. Xiao-Hong, Z. Xian-Zhou, Comput. Theor. Chem. 963 (2011) 34–39.
37. L. Padmaja, C. Ravikumar, D. Sajan, I. Hubert Joe, V.S. Jayakumar, G.R. Pettit, O.Faurskov Nielsen, J. Raman Spectrosc. 40 (2009) 419–428.
38. Obot I B, Obi-Egbedi N O and Umoren S A, Int J Electchem Sci., 2009; 4: 863-877.
39. I. Fleming, Frontier Orbitals and Organic Chemical Reactions, (John Wiley and Sons, NewYork, 1976
40. Obi-Egbedi N O, Obot I B, El-Khaiary M I, Umoren S A and Ebenso E E, Int J Electro Chem Sci., 2011; 6:5649-5675.
41. Hasanov R, Sadikglu M, and Bilgic S, Appl. Surf Sci, 2007; 253: 3913-3921.
42. T.A.Koopmans,Physica 1(1934)104-113.
43. Pearson R G, Inorg Chem, 1988; 27: 734-740.
44. K.K. Irikura, THERMO.PL, National Institute of Standards and Technology,Gaithersburg, MD, 2002.

\*\*\*\*\* \*\*\*\*\*